COMPETING FINANCIAL INTERESTS
The authors declare no competing financial interests.

Published online at http://www.nature.com/naturecellbiology/
Reprints and permissions information is available online at http://npg.nature.com/reprintsandpermissions/

1. Martin, S. & Parton, R. G. Lipid droplets: a unified view of a dynamic organelle. *Nature Rev. Mol. Cell Biol.* **7**, 373–378 (2006).
2. Blanchette-Mackie, E. J. *et al.* Perilipin is located on the surface layer of intracellular lipid droplets in adipocytes. *J. Lipid Res.* **36**, 1211–1226 (1995).
3. Vock, R. *et al.* Design of the oxygen and substrate pathways. VI. structural basis of intracellular substrate supply to mitochondria in muscle cells. *J. Exp. Biol.* **199**, 1689–1697 (1996).
4. Liang, T. J. *et al.* Viral pathogenesis of hepatocellular carcinoma in the United States. *Hepatology* **18**, 1326–1333 (1993).
5. Moradpour, D., Englert, C., Wakita, T. & Wands, J. R. Characterization of cell lines allowing tightly regulated expression of hepatitis C virus core protein. *Virology* **222**, 51–63 (1996).
6. Deleersnyder, V. *et al.* Formation of native hepatitis C virus glycoprotein complexes. *J. Virol.* **71**, 697–704 (1997).
7. Kato, N. *et al.* Molecular cloning of the human hepatitis C virus genome from Japanese patients with non-A, non-B hepatitis. *Proc. Natl Acad. Sci. USA* **87**, 9524–9528 (1990).
8. Hijikata, M. & Shimotohno, K. [Mechanisms of hepatitis C viral polyprotein processing]. *Uirusu* **43**, 293–298 (1993).
9. Dubuisson, J., Penin, F. & Moradpour, D. Interaction of hepatitis C virus proteins with host cell membranes and lipids. *Trends Cell Biol.* **12**, 517–523 (2002).
10. Wakita, T. *et al.* Production of infectious hepatitis C virus in tissue culture from a cloned viral genome. *Nature Med.* **11**, 791–796 (2005).
11. Lindenbach, B. D. *et al.* Complete replication of hepatitis C virus in cell culture. *Science* **309**, 623–626 (2005).
12. Zhong, J. *et al.* Robust hepatitis C virus infection in vitro. *Proc. Natl Acad. Sci. USA* **102**, 9294–9299 (2005).
13. Pietschmann, T. *et al.* Construction and characterization of infectious intragenotypic and intergenotypic hepatitis C virus chimeras. *Proc. Natl Acad. Sci. USA* **103**, 7408–7413 (2006).
14. Moriya, K. *et al.* Hepatitis C virus core protein induces hepatic steatosis in transgenic mice. *J. Gen. Virol.* **78**, 1527–1531 (1997).
15. Hope, R. G., Murphy, D. J. & McLauchlan, J. The domains required to direct core proteins of hepatitis C virus and GB virus-B to lipid droplets share common features with plant oleosin proteins. *J. Biol. Chem.* **277**, 4261–4270 (2002).
16. Egger, D. *et al.* Expression of hepatitis C virus proteins induces distinct membrane alterations including a candidate viral replication complex. *J. Virol.* **76**, 5974–5984 (2002).
17. Miyanari, Y. *et al.* Hepatitis C virus non-structural proteins in the probable membranous compartment function in viral genome replication. *J. Biol. Chem.* **278**, 50301–50308 (2003).
18. Quinkert, D., Bartenschlager, R. & Lohmann, V. Quantitative analysis of the hepatitis C virus replication complex. *J. Virol.* **79**, 13594–13605 (2005).
19. Tauchi-Sato, K., Ozeki, S., Houjou, T., Taguchi, R. & Fujimoto, T. The surface of lipid droplets is a phospholipid monolayer with a unique fatty acid composition. *J. Biol. Chem.* **277**, 44507–44512 (2002).
20. Londos, C., Brasaemle, D. L., Schultz, C. J., Segrest, J. P. & Kimmel, A. R. Perilipins, ADRP, and other proteins that associate with intracellular neutral lipid droplets in animal cells. *Semin. Cell Dev. Biol.* **10**, 51–58 (1999).
21. Blight, K. J., McKeating, J. A. & Rice, C. M. Highly permissive cell lines for subgenomic and genomic hepatitis C virus RNA replication. *J. Virol.* **76**, 13001–13014 (2002).
22. Klein, K. C., Dellos, S. R. & Lingappa, J. R. Identification of residues in the hepatitis C virus core protein that are critical for capsid assembly in a cell-free system. *J. Virol.* **79**, 6814–6826 (2005).
23. Owsianka, A. *et al.* Monoclonal antibody AP33 defines a broadly neutralizing epitope on the hepatitis C virus E2 envelope glycoprotein. *J Virol* **79**, 11095–11104 (2005).
24. Ishii, N. *et al.* Diverse effects of cyclosporine on hepatitis C virus strain replication. *J. Virol.* **80**, 4510–4520 (2006).
25. Lohmann, V., Korner, F., Herian, U. & Bartenschlager, R. Biochemical properties of hepatitis C virus NS5B RNA-dependent RNA polymerase and identification of amino acid sequence motifs essential for enzymatic activity. *J Virol* **71**, 8416–8428 (1997).
26. Ohsaki, Y., Maeda, T. & Fujimoto, T. Fixation and permeabilization protocol is critical for the immunolabeling of lipid droplet proteins. *Histochem. Cell Biol.* **124**, 445–452 (2005).

nature
cell biology

Supplementary Figures and legends

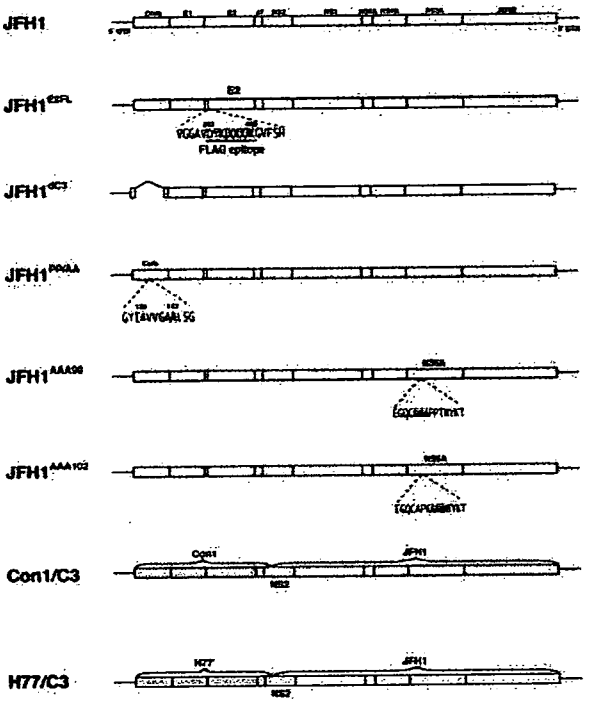

Supplementary Fig. 1

Schematic structures of HCV genomes and mutants used in this study

In JFH1^{E2FL}, the amino acid residues at positions 393 to 400 in the hyper variable region 1 of E2 were converted to a Flag epitope: DYKDDDDK. The JFH1^{E2FL} genome was used to generate other mutant variants of JFH1. In these cases the Flag epitope is marked with a blue vertical line. JFH1^{dC3} carried a deletion in the Core gene that eliminated the 17th to the 163rd amino-acid residue of Core. JFH1$^{PP/AA}$ is a mutant of JFH1^{E2FL} carrying alanine substitutions for proline residues at amino-acid positions 138 and 143 in Core. JFH1^{AAA99} and JFH1^{AAA102} contained mutated NS5A genes carrying triple-alanine substitutions for the APK sequence at amino acid positions 99 to 101 and the PPT sequence at amino acid positions 102 to 104, respectively. Constructs Con1/C3 and H77/C3 are chimeras in which the region from Core to the N-terminal domain of NS2 of JFH1 was replaced by the analogous region of the genotype 1b isolate Con1 or by the genotype 1a isolate H77[6].

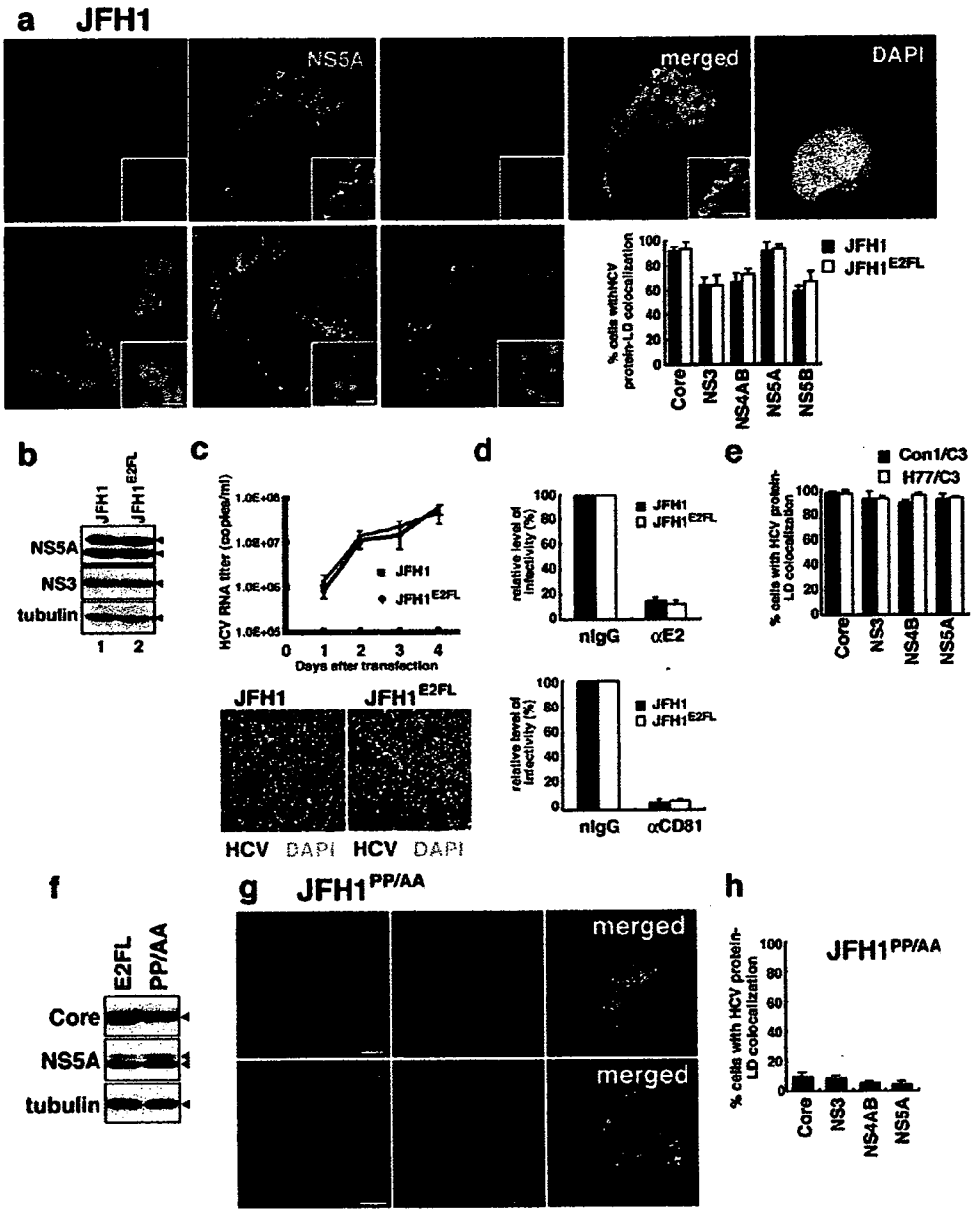

Supplementary Fig. S2 Kunitata Shimotohno NCB-S11732B

Supplementary Fig. 2 Characterization of mutant JFH1s

(a) JFH1-replicating cells were stained with indicated antibodies, BODYPI 493/503 and

DAPI. Scale bars = 2 μm. Percentages of JFH1- and JFH1^{E2FL}-replicating cells with overlapping signals for LDs and HCV proteins (n > 200). (b) HCV proteins in JFH1 and JFH1^{E2FL} replicating cells were analyzed by western blotting with indicated antibodies. (c) Efficiency of virus production and infectivity of JFH1 and JFH1^{E2FL} viruses were analyzed as described in Fig. 4. (n = 3) (d) Inhibition of HCV infection by anti-E2 antibody and anti-CD81 antibody. JFH1 and JFH1^{E2FL} virus were pre-incubated with normal IgG (nIgG) or anti-E2 antibody for 1 hr at 4°C and were subsequently used to inoculate Huh-7.5 cells (upper panel). Huh-7.5 cells were pre-incubated with normal IgG (nIgG) or anti-CD81 antibody for 1 hr at 37°C before inoculation with JFH1 or JFH1^{E2FL} viruses (lower panel) (n = 3). No obvious difference with respect to the subcellular localization of viral proteins (a), efficiency of viral replication (b), virus production (c), and pathway of virus entry (d) were observed between JFH1^{E2FL} and JFH1 (e) Con1/C3 or H77/C3 replicating cells were stained for HCV antigens (Core or NS3 or NS4B or NS5A) and LDs. The graphs show the percentage of Con1/C3 (black) or H77/C3 (white) positive cells in which HCV protein signals overlapped with LD signals. The overlapping signals were detected by using the ImageJ RG2B software package (n > 200). (f) Whole-cell extracts of JFH1^{E2FL} (E2FL) and JFH1$^{PP/AA}$ (PP/AA) replicon-bearing cells were analyzed by Western blot with indicated antibodies. Both Core^{Wt} and Core$^{PP/AA}$ had an apparent molecular weight of about 21 kDa, indicating that Core$^{PP/AA}$ was efficiently processed. The expression level of Core$^{PP/AA}$, however, was slightly lower than that of Core^{Wt}. (g) Analysis of the subcellular localization of Core and NS5A in cells bearing the JFH1$^{PP/AA}$ mutant. Cells were labeled to detect LDs (green), Core (red), NS5A (red) and nuclei DAPI (blue). Scale bars = 10μm. (h) The percentages of JFH1$^{PP/AA}$ replicon-bearing cells positive for overlapping signals of LDs and HCV proteins are indicated (n > 200).

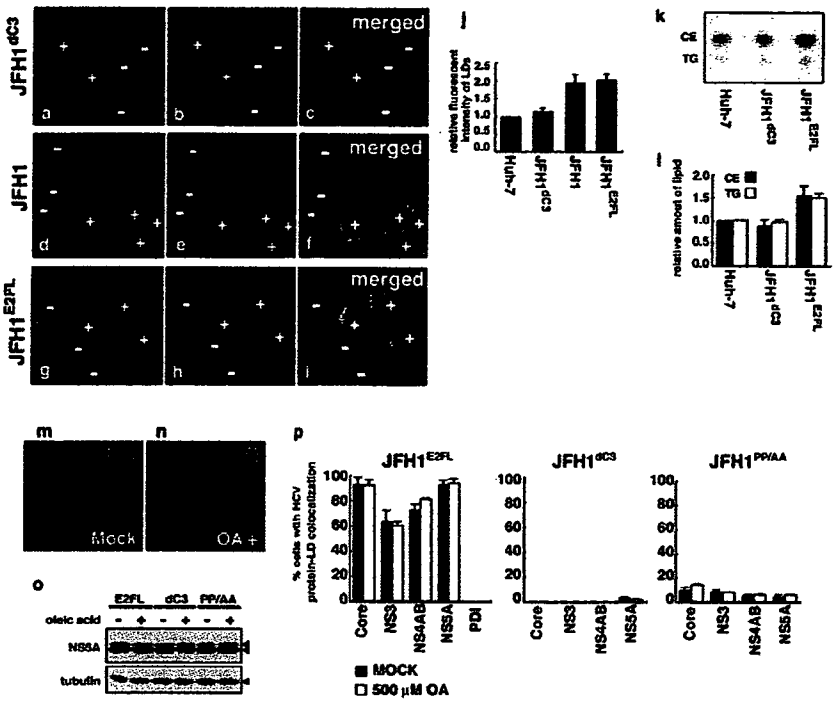

Supplementary Fig. S3 Kunitata Shimotohno
NCB-S11732B

Supplementary Fig. 3

Enhanced formation of LDs in JFH1- and JFH1^{E2FL}-replicating cells

Cells transfected with JFH1^{dC3} (a-c), JFH1 (d-f), and JFH1^{E2FL} RNA (g-i) were stained with BODIPY493/503 (green), DAPI (blue), and anti-NS5A antibody (red). + and – indicate HCV-positive and HCV-negative cells, respectively. Fluorescence intensities of LDs in Huh-7 cells, JFH1^{dC3}-, JFH1-, and JFH1^{E2FL}-replicating cells were measured by confocal microscopy. The results are represented as relative fluorescence intensity of LDs (j). (k and l) Lipid fraction extracted from Huh-7 cells, JFH1^{dC3}-, and JFH1^{E2FL}-replicating cells was analyzed by thin-layer chromatography. Each lane was loaded with lipid corresponding to an equal amount of protein. Cholesterol ester (CE) and triglyceride (TG) are indicated (k). The relative intensity of CE and TG in panel k is shown in l (n = 3). (m-p) JFH1^{E2FL} replicon-bearing cells were treated with 500 μM oleic acid for 24 hrs and were labeled with BODIPY493/503 (m and n). Cells transfected with JFH1^{E2FL} (E2FL), JFH^{dC3} (dC3), or JFH$^{PP/AA}$ (PP/AA) RNA were treated with or without oleic acid. (o) The HCV protein level as represented by the level of NS5A was analyzed by western blot. (p) The percentages of cells positive for overlapping signals for LDs and the HCV proteins or PDI are indicated. The data was obtained in the presence (500 μM) or absence (MOCK) of oleic acid in the culture medium (n > 200).

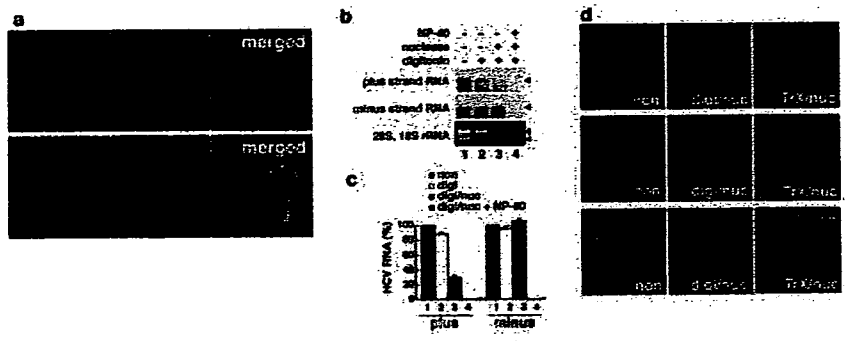

Supplementary Fig. S4 Kunitada Shimotohno
NCB-S11732B

Supplementary Fig. 4

Subcellular localizations of plus- and minus-strand HCV RNA

(a) JFH1^{E2FL} replicating cells were analyzed by *in situ* hybridization to detect plus- and minus-strand HCV RNA (green). The cells were also labeled with anti-PDI antibodies (red) and DAPI (blue). Scale bars = 10 μm. (b, c) Relative amounts of plus- and minus-strand HCV RNAs. JFH1^{E2FL}-expressing cells were permeabilized with digitonin. The cells were treated with nuclease in the presence or absence of NP-40. Then, total RNA was analyzed by Northern blots with strand-specific HCV RNA probes. 28S and 18S ribosomal RNA was stained with ethidium bromide (b). The signals were quantified and plotted in c (n = 3). The amounts of plus- and minus-strand RNA were similar before and after digitonin treatment (lanes 1 and 2). The level of plus-strand RNA, however, was reduced by approximately 70% after nuclease treatment, whereas the level of minus-strand RNA remained constant (lanes 2 and 3). Nuclease treatment in the presence of NP-40 used to lyse the membranes caused both plus- and minus-strand HCV RNA to disappear (lane 4). This result suggests that ~30% and ~100% of plus- and minus-strand HCV RNA, respectively, are located in the replication complexes. (d) Localization of nuclease-resistant JFH1^{E2FL} RNA was analyzed by *in situ* hybridization. Digitonin-permeabilized cells were treated with nuclease in the presence (TrX/nuc) or absence (digi/nuc) of Triton X-100. Total RNA was visualized with SYTO RNAselect. "non" indicates cells without digitonin and nuclease treatment. Using the nuclease-resistant HCV RNA as a marker of replication complexes, we examined the localization of the replication complexes. Both plus- and minus-strand HCV RNA were detected in the perinuclear region even after the nuclease treatment. As expected, these RNAs were no longer detectable after nuclease treatment in the presence of Triton X-100. The intensity of the plus-strand RNA signal decreased after nuclease treatment (compare upper left and middle panels). However, the intensity of the minus-strand RNA signal remained unchanged after the treatment. These results correlated with the data obtained by Northern blotting analysis. For this reason, the percentages of cells with overlapping signals for LDs and plus- or minus-strand HCV RNA (Fig. 2c) were measured after lysis of cells with digitonin and nuclease treatment. Scale bars = 10 μm.

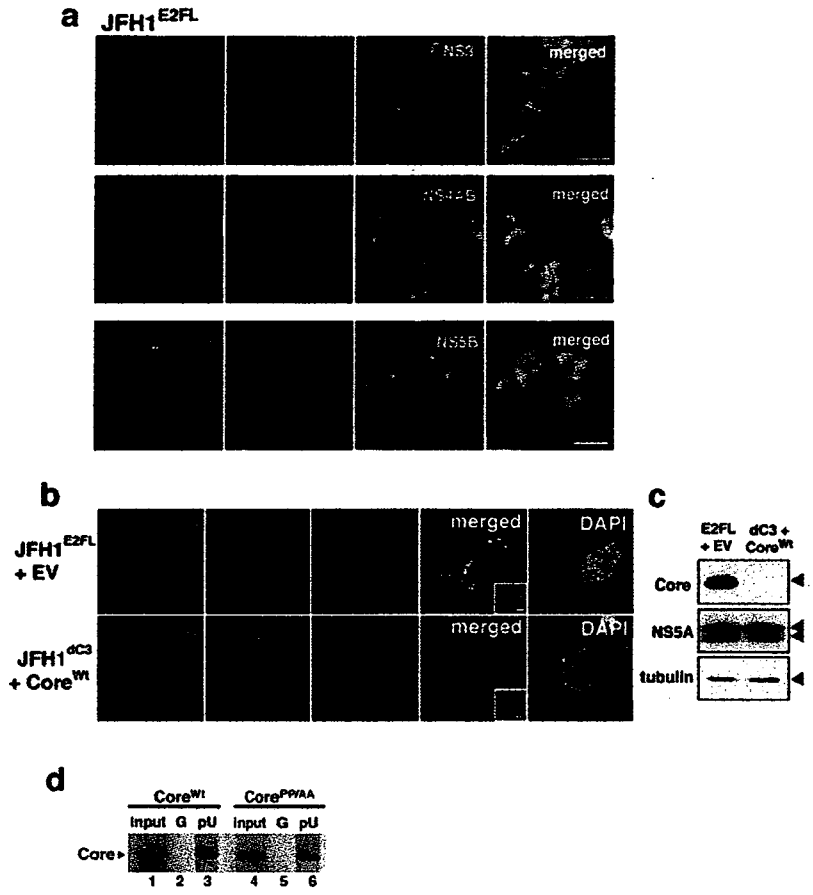

Supplementary Fig. S5 Kunitata Shimotohno NCB-S11732B

Supplementary Fig. 5

Subcellular localization of HCV proteins in JFH1^{E2FL}-replicating cells and cells inoculated with rescued viruses, and RNA binding nature of Core.

(a) JFH1^{E2FL}-replicating cells were labeled to detect LDs (green), Core (red), NS3 (cyan), NS4AB (cyan), and NS5B (cyan). Scale bars = 2 μm (b) The subcellular localizations of NS5A and Core in Huh-7.5 cells infected with viruses released from JFH1^{E2FL} replicon-bearings cells co-transfected with pcDNA3 (upper panels) and from JFH1^{dC3} replicon-bearing cells co-transfected with pcDNA3-Core^{Wt} (lower panels). Cells were labeled with DAPI (white), BODIPY 493/503 (green), anti-Core (blue), and anti-NS5A (red) antibodies. The insets are high magnifications of the corresponding panel. (c) HCV proteins from these infected cells were analyzed by western blotting. (d) An RNA-protein binding precipitation assay was performed with *in vitro*-translated and ^{35}S-radiolabeled Core^{Wt} (lane 1-3) and Core$^{PP/AA}$ (lane 4-6). The resulting precipitates were analyzed by SDS-PAGE and detected by autoradiography. "G" and "pU" mark samples obtained using protein G Sepharose and poly-U Sepharose as the resin, respectively. "input" indicates 1/20 of the amount of translated product used in this assay.

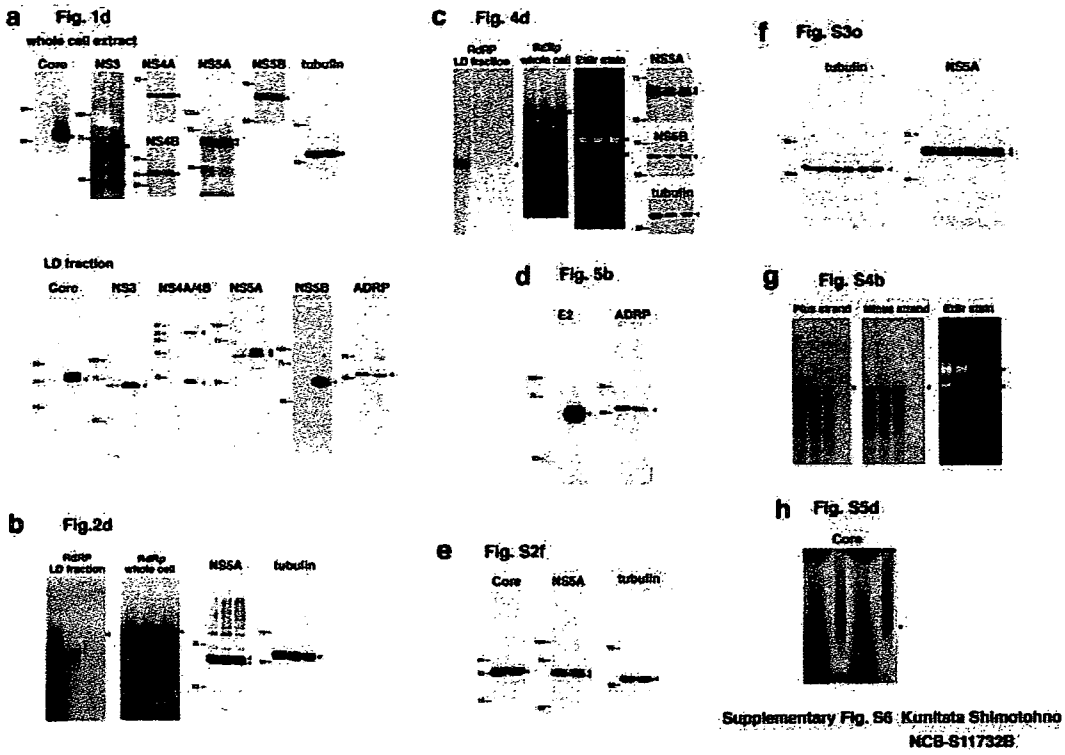

Supplementary Fig. 6

Full scan of key gel images depicted in the individual figures.

Full scans of (a) immunoblot detection of whole cell extract and LD fraction from JFH1^{E2FL}- and JFH1^{dC3}-replicating cells shown in Fig. 1d, (b) RNA synthesis assay and immunoblot detection of JFH1^{E2FL}-, JFH1^{dC3}-, and JFH1$^{PP/AA}$-replicating cells shown in Fig. 2d, (c) RNA synthesis assay and immunoblot detection of JFH1^{E2FL}-, JFH1^{AAA99}-, and JFH1^{AAA102}-replicating cells shown in Fig. 4d, (d) immunoblot detection of LD fraction from JFH1^{E2FL}- and JFH1^{dC3}-replicating cells shown in Fig. 5b, (e) immunoblot detection of JFH1^{E2FL}- and JFH1$^{PP/AA}$-replicating cells shown in Fig. S2f, (f) immunoblot detection of JFH1^{E2FL}-replicating cells shown in Fig. S3o, (g) Northern Blotting analysis of JFH1^{E2FL}-replicating cells shown in Fig. S4b, and (h) RNA-protein binding precipitation assay shown in Fig. S5d. Size of molecular weight markers (kDa) is indicated at the left side of western blot gel images. *In vitro* transcribed HCV RNA was used as a size marker for RNA gel electrophoresis (b, c, and g).

plasmid name	primer sequences (5' to 3')	template for PCR	restriction enzyme	original plasmid
pcDNA3-Core ^{1a}	AGAGCCAAGCTTCACCATGAGCACAAATCCTAAACC	pJFH1	HindIII	pcDNA3
	AATGGAATTCTCAAGCAGAGACCGGAACGGTGATGC		EcoRI	
pcDNA3-TME2	AGACCCAAGCTTCACCATGGCTCACTGGGGCGTCATGTTC	pJFH1	HindIII	pcDNA3
	AATGCAATTCTCATCCTTCGCGCCTCCCCCAACAAG		EcoRI	
pcDNA3-NS3	AGACCCAAGCTTCACCATGGCTCCCATCACTGCTTATGCC	pJFH1	HindIII	pcDNA3
	AATGGAATTCTCAGGTCATGACCTCAAGGTCAGC		EcoRI	
pcDNA3-NS4B	AGACCCAAGCTTCACCATGGCCTCTAGGGCGGCTCTCATCG	pJFH1	HindIII	pcDNA3
	AATGGAATTCTCAGCATGGGATGGGGCAGTCCTC		EcoRI	
pcDNA3-NS5B	CTCGGATCCACCATGTCCATGTCATACTCCTGGACC	pJFH1	BamHI	pcDNA3
	AATGGAATTCCTACCGAGCGGGGGAGTAGGAAGAGG		EcoRI	
pcDNA3-Core $^{PP/AA}$	CATGGGGTACATCGCCGTCGTAGGCGCCGCGCTTAGTGGCG	pJFH1 $^{PP/AA}$	HindIII	pcDNA3
	CGCCACTAAGCGCGGCGCCTACGACGGCGATGTACCCCATG		EcoRI	
pJFH1 ^{E2FL}	GATTACAAGGATGACGACGATAAGGGCGTGTTCAGCCATGGCCC	pJFH1	BsiWI	pJFH1
	CTTATCGTCGTCATCCTTGTAATCAACAGCGCCTCCAACGGTGG		NotI	
	CGCACATGATGATGAACTGG			
	GTAATGTCAAACACCACACC			
pJFH1 $^{dC-2}$	GAAAAACCAAAAGAAACACCAACTATGCAACAGGGAACCTACC	pJFH1 ^{E2FL}	EcoRI	pJFH1 ^{E2FL}
	GTTGGTGTTTCTTTTGGTTTTTC		BsiWI	
	CGGACATGATGATGAACTGG			
	GTAATGTCAAACACCACACC			
pJFH1 $^{PP/AA}$	CATGGGGTACATCGCCGTCGTAGGCGCCGCGCTTAGTGGCG	pJFH1 ^{E2FL}	EcoRI	pJFH1 ^{E2FL}
	CGCCACTAAGCGCGGCGCCTACGACGGCGATGTACCCCATG		BsiWI	
	CGGACATGATGATGAACTGG			
	GTAATGTCAAACACCACACC			
pJFH1 ^{E2FL} dBamHI	TACTGCCTGGCATCCTGTCTCC	pJFH1 ^{E2FL}	NsiI	pJFH1 ^{E2FL}
	GGAGACAGGATGCCAGGCAGTA		RsrII	
	GTATTACCAATGAGGTGACC			
	GAACAATTTAGAGGTCAGCC			
pJFH1 ^{AAA99}	GGCCAGTGCGCGGCGGCACCCCCCACG	pJFH1 ^{E2FL}	BamHI	pJFH1 ^{E2FL} dBamHI
	CGTGGGGGGTGCCGCCGCGCACTGGCC		RsrII	
	TGGATGAACAGGCTTATTGC			
	GGTTGAAGCTCTACCTGATC			
pJFH1 ^{AAA102}	GCGCCGAAAGCCGCCGCGAACTACAAG	pJFH1 ^{E2FL}	BamHI	pJFH1 ^{E2FL} dBamHI
	CTTCTAGTTCCCCGCCGCCTTTCGCCCC		RsrII	
	TGGATGAACAGGCTTATTGC			
	GGTTGAAGCTCTACCTGATC			

Supplementary Table

A list of the plasmids used in this work. The sets of primers used to amplify the target genes, the template plasmids used in the PCRs, the restriction sites, and plasmids into which the amplified DNA fragments were inserted are shown.

Supplementary Materials and Methods

Cell culture

The human hepatoma cell lines Huh-7 and Huh-7.5[1] were grown in Dulbecco's modified Eagle's medium (DMEM; Invitrogen, CA, USA) supplemented with 10% fetal bovine serum (FBS), 100 U/ml nonessential amino acids (Invitrogen), and 100 μg/ml penicillin and streptomycin sulfate (Invitrogen). Huh-7.5 cells were obtained from Dr. C. Rice. (Rockefeller University, USA)

Plasmid construction

All plasmids were generated by insertion of PCR-amplified fragments into expression plasmids. The plasmids, the primer sequences, templates for the PCRs, and the restriction enzyme sites used to construct the plasmids are listed in Supplementary Table 1.

DNA and RNA transfection

Transfection of HCV RNA was performed as previously described[2]. DNA transfection was performed using Lipofectamine 2000 (Invitrogen) according to the manufacturer's instructions.

Northern blotting

Northern blot analysis was performed as described previously[3] with strand specific RNA probes.

RT-PCR analysis

Quantitative real-time RT-PCR analysis of the HCV RNA titer was performed as described previously[4].

ELISA for the detection of Core

Core in the culture medium was quantified with an ELISA according to the manufacturer's protocol (HCV antigen ELISA test, Ortho-Clinical Diagnostics).

Thin-layer chromatography

Lipid samples extracted from cells were dissolved in chloroform methanol and were

subjected to thin-layer chromatography with a high-performance TLC plate (Merck) by the two-step method[5]. The plate was charred by a copper acetate phosphoric acid solution at 180°C.

***In vitro* transcription**

RNA for transfection was synthesized using MEGAscript T7 (Ambion, TX, USA). Plasmids carrying the JFH1 RNA sequence were linearized with *Xba*I and used as templates for transcription. Probes for *in situ* hybridization were synthesized using MAXIscript Sp6 or T7 (Ambion) in the presence of the DIG RNA labeling mix (Roche). Probes for Northern blots were synthesized with MAXIscript Sp6 or T7 in the presence of 1.85 MBq of [α-^{32}P] UTP (Amersham Biosciences). For detection of plus-strand HCV RNA, minus-strand RNA probes were generated using pcDNA3-TME2 (*Hin*dIII for linearization), pcDNA3-NS3 (*Hin*dIII), and pcDNA3-NS5B (*Bam*HI) as templates for *in vitro* transcription. For detection of minus-strand HCV RNA, plus-strand RNA probes were generated using pcDNA3-TME2 (*Eco*RI), pcDNA3-NS3 (*Xba*I), and pcDNA3-NS5B (*Bam*HI) as templates. The RNA probes used for *in situ* hybridization were subjected to alkaline hydrolysis to generate fragments of ~170 nucleotides in length. Synthesized RNA probes were treated with DNase I (Ambion) and size fractionated using MicroSpin G-50 columns (Amersham Biosciences).

Sucrose density gradient centrifugation of culture medium

The 100-time concentrated medium from JFH1-bearing cells was loaded onto 20-50% [w/v] sucrose gradient containing 50 mM Hepes-KOH (pH 7.4), 100 mM NaCl and 1mM EDTA followed by centrifugation at 100,000 x g for 16 hrs using RPS40T rotor of HITACHI ultracentrifuge. The gradient was fractionated into 31 fractions. Buoyant density of each fraction was analyzed by Abe refractometer (ATAGO Inc., Japan). Each fraction was dialyzed against serum free DMEM and was used for the infection experiment as well as quantification of Core and HCV RNA titer as described above.

Infection experiments

Cells were cultured in DMEM containing 5% FBS. The medium was collected and mixed with a 0.01 volume of 1 M HEPES (pH 7.4). After filtering the sample through a 0.22-μm filter (Millipore), the filtrate was concentrated by reducing the volume to

between 1/50 and 1/100 of the original volume with an Amicon Ultra-15 centrifugal filter with Ultracel-100 membrane (Millipore). Huh-7.5 cells seeded on a collagen-coated Labtech II 8-well chamber were incubated with 100 µl of the concentrated medium for 120 min. Then, the cells were washed three times with DMEM. Twenty-four hours after the inoculation, the cells were labeled with serum from HCV-infected patients to determine the infectivity level.

***In situ* hybridization analysis**

Huh-7 cells transfected with JFH1 RNA were seeded on a collagen-coated Labtech II 8-well chamber (Nunc). Three days after seeding, the cells were washed twice with PBS and fixed with fixation solution for 15 min at room temperature. Then, the cells were permeabilized with 0.05% Triton X-100 in fixation solution for 15 min at room temperature. After washing the cells twice with cold DEPC-treated PBS, the cells were incubated in 95% formamide and 0.1x SSC (1x SSC: 150 mM NaCl and 15 mM sodium citrate) for 15 min at 65°C. After chilling the chamber on ice, the cells were incubated in 100 µl of pre-hybridization solution for 60 min at room temperature. Pre-hybridization solution was composed of 50% formamide, 2x SSC, 1 µg/ml of salmon sperm DNA (sonicated to 1-2 kb pieces, Roche), 1 µg/ml of yeast tRNA (Roche), and 2 mM vanadyl ribonucleoside complex (NEB). Then, the cells were incubated in 100 µl of hybridization solution (pre-hybridization solution containing 10% dextran sulfate and 100 to 500 ng/ml of the RNA probes) for 40 hrs at 42°C. After the hybridization, the slide glass in the chamber was transferred to a bucket filled with wash solution 1 (50% formamide and 2x SSC at pH 7.4) and washed three times for 20 min at 50°C with gentle agitation. Then, the slide was washed three more times in wash solution 2 (0.1x SSC at pH 7.4) for 20 min at 50°C with gentle agitation. The slide was incubated in blocking solution for 30 min at room temperature. To detect DIG-labeled probes, sheep anti-DIG antibodies (Roche) and Alexa 488 or Alexa 568 anti-sheep IgG antibodies (Invitrogen) were used as primary and secondary antibodies, respectively. When HCV RNA, Core, and NS5A were simultaneously labeled in the same sample, anti-DIG antibodies and the Alexa-conjugated antibodies were incubated with the samples separately to avoid cross-reaction of the Alexa 488 or Alexa 568 anti-sheep IgG antibodies with mouse and rabbit IgG. Briefly, the incubation with the anti-DIG antibodies and the Alexa 488 anti-sheep IgG antibodies was performed first. After

washing with PBS followed by a second fixation procedure, the cells were incubated with anti-Core and anti-NS5A antibodies followed by Alexa 568 anti-rabbit IgG and Alexa 647 anti-mouse IgG antibodies. For treatment with nuclease, digitonin-permeabilized cells were treated with 1 μg/ml of RNase A in the presence or absence of 0.05% Triton X-100 for 15 min at 37°C. After the treatment, RNase A was inactivated by incubation with 4% formaldehyde. Then, the cells were completely permeabilized with 0.05% Triton X-100 for 5 min at room temperature.

Statistical analysis of the recruitment of viral components to the LD

Only the cells that have any LDs surrounded by HCV proteins, PDI, or HCV RNA were counted as positive under immunofluorescence microscopy, and those adjacent to HCV signal were not included. The obtained cell number was divided by the total number of HCV replicating cells and is shown as "% cells with HCV protein-LD colocalization". In case of the chimeras Con1/C3 and H77/C3 LD colocalization with HCV proteins was additionally analyzed by using the ImageJ RG2B software package (Rasband, W.S., ImageJ, U. S. National Institutes of Health, Bethesda, Maryland, USA, http://rsb.info.nih.gov/ij/, 1997-2006.). Approximately 200 cells were examined for each antigen.

RNA-protein binding precipitation assay

In vitro translated [^{35}S]-labeled products (Core^{Wt} and Core$^{PP/AA}$) were incubated with poly-U or protein G Sepharose resin in 50 mM HEPES (pH7.4), 100 mM NaCl, 0.1 % NP-40, and RNase inhibitor at 4°C for 2 hrs. After five washes, resin-bound radiolabeled proteins were analyzed by gel electrophoresis followed by autoradiography.

Supplementary References

1. Blight, K. J., McKeating, J. A. & Rice, C. M. Highly permissive cell lines for subgenomic and genomic hepatitis C virus RNA replication. *J Virol* **76**, 13001-14 (2002).
2. Lohmann, V. et al. Replication of subgenomic hepatitis C virus RNAs in a hepatoma cell line. *Science* **285**, 110-3 (1999).
3. Miyanari, Y. et al. Hepatitis C virus non-structural proteins in the probable membranous compartment function in viral genome replication. *J Biol Chem* **278**, 50301-8 (2003).
4. Takeuchi, T. et al. Real-time detection system for quantification of hepatitis C virus genome. *Gastroenterology* **116**, 636-42 (1999).
5. Tauchi-Sato, K., Ozeki, S., Houjou, T., Taguchi, R. & Fujimoto, T. The surface of lipid droplets is a phospholipid monolayer with a unique Fatty Acid composition. *J Biol Chem* **277**, 44507-12 (2002).
6. Pietschmann, T. et al. Construction and characterization of infectious intragenotypic and intergenotypic hepatitis C virus chimeras. *Proc Natl Acad Sci U S A* **103**, 7408-13 (2006).

ELSEVIER

Journal of Hepatology 46 (2007) 26–36

Journal of Hepatology

www.elsevier.com/locate/jhep

Serum-derived hepatitis C virus infectivity in interferon regulatory factor-7-suppressed human primary hepatocytes

Hussein H. Aly[1,2,3], Koichi Watashi[2], Makoto Hijikata[2], Hiroyasu Kaneko[2], Yasutugu Takada[1], Hiroto Egawa[1], Shinji Uemoto[1], Kunitada Shimotohno[2,*]

[1]*Graduate School of Medicine, Department of Transplant Surgery, Kyoto University Hospital, Kyoto, Japan*
[2]*Laboratory of Human Tumor Viruses, Institute of Virus Research, Kyoto University, Japan*
[3]*Hepatology Department, National Hepatology and Tropical Medicine Research Institute, Cairo, Egypt*

See Editorial, pages 1–5

***Background/Aims*: The development of an efficient in vitro infection system for HCV is important in order to develop new anti-HCV strategy. Only Huh7 hepatocyte cell lines were shown to be infected with JFH-1 fulminant HCV-2a strain and its chimeras. Here we aimed to establish a primary hepatocyte cell line that could be infected by HCV particles from patients' sera.**

***Methods*: We transduced primary human hepatocytes with human telomerase reverse transcriptase together with human papilloma virus 18/E6E7 (HPV18/E6E7) genes or simian virus large T gene (SV40 T) to immortalize cells. We also established the HPV18/E6E7-immortalized hepatocytes in which interferon regulatory factor-7 was inactivated. Finally we analyzed HCV infectivity in these cells.**

***Results*: Even after prolonged culture HPV18/E6E7-immortalized hepatocytes exhibited hepatocyte functions and marker expression and were more prone to HCV infection than SV40 T-immortalized hepatocytes. The susceptibility of HPV18/E6E7-immortalized hepatocytes to HCV infection was further improved, in particular, by impairing signaling through interferon regulatory factor-7.**

***Conclusions*: HPV18/E6E7-immortalized hepatocytes are useful for the analysis of HCV infection, anti-HCV innate immune response, and screening of antiviral agents with a variety of HCV strains.**

***Keywords*: Immortalization; Primary hepatocytes; HCV infection; IRF-7; IRF-3; HPV18/E6E7; Innate immune response**

1. Introduction

Infection with Hepatitis C virus (HCV) is a serious problem worldwide since 3% of the world's population is chronically infected [1]. Chronic HCV may lead to liver cirrhosis and hepatocellular carcinoma. Current standard therapy utilizes the combination of pegylated interferon-α and ribavirin, which results in a sustained response in only 30–60% of patients [2–5]. Many patients, however, do not qualify for or tolerate standard therapy [6]. Thus, it is important to develop an efficient in vitro infection system for HCV to facilitate the discovery of new anti-HCV strategies. Only Huh7 cell line is permissive for replication, infection and release of the fulminant hepatitis-derived HCV-2a (JFH-1) *strain* and its chimeric derivatives [7–9]. No other hepatocyte cell lines are able to support HCV replication efficiently.

Received 5 June 2006; received in revised form 24 July 2006; accepted 1 August 2006; available online 30 October 2006

* Corresponding author. Tel.: +81 75 751 4000; fax: +81 75 751 3998.
E-mail address: kshimoto@virus.kyoto-u.ac.jp (K. Shimotohno).

0168-8278/$32.00
doi:10.1016/j.jhep.2006.08.018

Normal human hepatocytes are the ideal system in which to study HCV infectivity. When cultured in vitro, however, they proliferate poorly and divide only a few times [10]. Continuous proliferation could be achieved however by introducing oncogenes, such as Simian virus large tumor antigen (SV40 T) [11]. This often resulted in tumor development [12] together with numerical (aneuploidy) and structural (aberrations) chromosome abnormalities [13]. The human papilloma virus E6E7 genes (HPV/E6E7) immortalized multiple cell types that were phenotypically and functionally similar to the parental cells [14–20]. As yet, no human hepatocytes have been immortalized with HPV18/E6E7.

We established a human primary non-neoplastic hepatocyte cell line transduced with the HPV18/E6E7 that retained primary hepatocyte characteristics even after prolonged culture, and were more prone to HCV infection than those cells immortalized with SV40 T antigen. We further improved the susceptibility of HPV18/E6E7-immortalized hepatocytes to HCV infectivity by impairing interferon regulatory factor-7 (IRF-7) expression. These cells are useful to assay infectivity of HCV strains other than JFH-1, HCV replication, innate immune system engagement of HCV, and screening of anti-HCV agents. This infection system using non-neoplastic cells also suggested that IRF-7 plays an important role in eliminating HCV infection.

2. Materials and methods

2.1. Cell cultures

We obtained the approval of the Ethical Committee of Kyoto University for the use of human hepatocytes and sera obtained from HCV-positive patients. Informed consent was obtained from both the hepatocyte donor and HCV-positive patients. Primary hepatocytes (P.H.) were cultured as described [21]. HeLa, 293, Huh-7.5, and PH5CH8 cells were cultured as previously described [22]. For three-dimensional (3D) cultures, Mebiol Gel (Mebiol Inc.) was prepared according to the manufacturer's instructions.

2.2. Plasmids construction

The SV40 T, hTERT and HPV/E6E7 fragments from pAct-SVT, PCX4neo/hTERT, and pLXSN-E6E7 plasmids were inserted into pCSII-EF-RFA plasmid creating the pCSII-EF-SVT, pCSII-EF-hTERT, and pCSII-EF-E6E7 plasmids, respectively. The full-length IRF-3 and IRF-7 genes were cloned by RT-PCR using total RNA isolated from 293 cells as a template and were inserted into pcDNA3 vector. Dominant-negative forms of IRF-3 (DNIRF-3) and IRF-7 (DNIRF-7) were constructed by PCR amplification of the coding region for amino acid residues 108–427 of IRF-3 and 237-514 of IRF-7, respectively. The amplified IRF-3 fragment was cloned into pcDNA3 in frame with a FLAG epitope tag generating pcFLAG-DNIRF-3. The amplified IRF-7 fragment was cloned into pLXSH in frame with HA epitope tag generating pLXSH-HA-DNIRF-7. The pIFNβ promoter-luc and pIFNα promoter-luc plasmids were gifts from Dr. Taniguchi of the Tokyo University. The psiRNA-hIRF-3 and psiRNA-hIRF-7 plasmids were purchased from Invivogen (USA).

2.3. Immunoblot analysis

Immunoblot analysis was performed as described previously [22]. We used anti-SV40 T (Santa Cruz), anti-HPV18/E7 (Santa Cruz), anti-tubulin (Sigma), anti-FLAG (Sigma), and anti-HA (Sigma) antibodies.

2.4. Transfection, small interfering RNA silencing and luciferase assays

Transfection of plasmid DNA was performed using Effectene transfection reagent (Qiagen) as recommended by the manufacturer. The pLXSH-HA-DNIRF-7 plasmid was transfected into the HuS-E/2 clone; transfectants were selected in 100 μg/ml hygromycin B (Gibco). The psiRNA-hIRF-3 and psiRNA-hIRF-7 plasmids were separately transfected into HuS-E/2 cells followed by Zeocin (250 μg/ml) selection. After two weeks of continuous selection, cells were infected with HCV. Luciferase assays were conducted as previously described [22]. The results are presented as relative light units (RLU) normalized to the total content of protein in the cell lysates.

2.5. Reverse transcriptase polymerase chain reaction (RT-PCR) and real-time RT-PCR

Using 250 ng of total RNA as a template, we performed RT-PCR with a one-step RNA PCR kit (Takara) according to the manufacturer's instructions. The primer sets and reaction conditions used are detailed in Table 1. To measure HCV-RNA titers by real-time RT-PCR, we collected RNA from infected wells. Five hundred nanograms of total cellular RNA was analyzed for the quantity of HCV-RNA as previously described [23].

2.6. HCV infection experiment

HCV infection experiment from serum was done as mentioned before [22]. HCV-infected-serums were titrated and 1×10^5 HCV-RNA copies/ml were used for each infection experiment. Concentrated culture medium for HCV/JFH1-producing cells was prepared as previously described [7]. HCV titer in the concentrated medium was measured, adjusted and added to the cells as mentioned above.

2.7. Blocking of HCV infectivity by anti-CD81

Inhibition of HCV infectivity was performed by blocking CD81 as previously described [7].

3. Results

3.1. Establishment of immortalized primary human hepatocytes

Primary hepatocytes were isolated from liver tissue obtained from a 9-year-old male patient with Primary Hyperoxaluria who had undergone liver transplantation. Hepatocytes were left unmanipulated or transduced with CSII-EF-hTERT alone or in combination with CSII-EF-SVT or CSII-EF-E6E7 to enhance the efficiency of immortalization. After six weeks only cells transduced by the combination of hTERT and either LT or HPV18/E6E7 continued to proliferate. Initially appearing colonies with a growth advantage were picked up and expanded. SV40 T-immortalized cell clones were named HuS-T cells and given numbers from 1 to 7,

Table 1
Primer sequences and RT-PCR parameters

Genes	Primer sequence 5′–3′	PCR parameters[a]
HGF	F: AGGAGCCAGCCTGAATGATGA R: CCCTCTGATGTCCCAAGATTAGC	95, 56, 72 1 min, 45 s, 1 min
TGFα	F: ATGGTCCCCTCGGCTGGA R: GGCCTGCTTCTTCTGGCTGGCA	95, 59, 72 45 s, 30 s, 1 min
TGFβ1	F: GCCCTGGACACCAACTATTGCT R: AGGCTCCAAATGTAGGGGCAGG	95, 58, 72 45 s, 30 s, 1 min
TGFβ2	F: GATTTCCATCTACAAGACCACGAGGGACTTGC R: CAGCATCAGTTACATCGAAGGAGAGCCATTCG	95, 58, 72 45 s, 30 s, 1 min
HGFR	F: TGGTCCTTGGCGTCGTCCTC R: CTCATCATCAGCGTTATCTTC	95, 54, 72 30 s, 45 s, 1 min
EGFR	F: CTACCACCACTCTTTGAACTGGACCAAGG R: TCTATGCTCTCACCCCGTTCCAAGTATCG	95, 58, 72 45 s, 30 s, 1 min
TGFβ1R	F: CGTGCTGACATCTATGCAAT R: AGCTGCTCCATTGGCATAC	95 s, 54, 72 30 s, 45 s, 1 min
TGFβ2R	F: TGCACATCGTCCTGTGGAC R: GTCTCAAACTGCTCTGAAGTGTTC	95, 58, 72 45 s, 30 s, 1 min
FGFR	F: ATGTGGAGCTGGAAGTGCCTC R: GGTGTTATCTGTTTCTTTCTCC	95, 54, 72 30 s, 45 s, 1 min
IGF-1R	F: ACCCGGAGTACTTCAGCGCT R: CACAGAAGCTTCGTTGAGAA	95, 54, 72 30 s, 45 s, 1 min
HNF1α	F: GTGTCTACAACTGGTTTGCC R: TGTAGACACTGTCACTAAGG	95, 52, 72 45 s, 30 s, 1 min
HNF1β	F: GAAACAATGAGATCACTTCCTCC R: CTTTGTGCAATTGCCATGACTCC	95, 52, 72 1 m, 45 s, 1 min
HNF3β	F: CACCCTACGCCTTAACCAC R: GGTAGTAGGAGGTATCTGCGG	95, 56, 72 1 m, 45 s, 1 min
HNF4	F: CTGCTCGGAGCCACAAAGAGATCCATG R: ATCATCTGCCACGTGATGCTCTGCA	95, 58, 72 45 s, 30 s, 1 min
Albumin	F: AGTTTGCAGAAGTTTCCAAGTTAGTG R: AGGTCCGCCCTGTCATCAG	95, 55, 72 45 s, 30 s, 1 min
Apolipoprotein-a	F:AGGCTCGGCATTTCTGGCAG R: TATCCCAGAACTCCTGGGTC	95, 55, 72 45 s, 30 s, 1 min
HTF	F: TCGCTACAGCCTTTGCAATG R: TTGAGGGTACGGAGGAGTTCC	95, 55, 72 45 s, 30 s, 1 min
E-cadherin	F: TCCATTTCTTGGTCTACGCC R: TTTGTCCTACCGACTTCCAC	95, 55, 72 45 s, 30 s, 1 min
CYP 1B1	F: CACCAAGGCTGAGACAGTGA R: GCCAGGTAAACTCCAAGCAC	94, 57, 72 30 s, 30 s, 1 min
CYP 2C9	F: GGACAGAGACGACAAGCACA R: TGGTGGGGAGAAGGTCAAT	94, 57, 72 30 s, 30 s, 1 min
CYP 2B	F: GGCACACAGCCAAGTTTACA R: CCAGCAAAGAAGAGCGAGAG	94, 57, 72 30 s, 30 s, 1 min
CYP 3A4	F: TGTGCCTGAGAACACCAGAG R: GCAGAGGAGCCAAATCTACC	94, 57, 72 30 s, 30 s, 1 min
CYP 2E1	F: CCGCAAGCATTTTGACTACA R: GCTCCTTCACCCTTTCAGAC	94, 57, 72 30 s, 30 s, 1 min
CYP 1A1	F: AGGCTTTTACATCCCCAAGG R: GCAATGGTCTCACCGATACA	94, 57, 72 30 s, 30 s, 1 min
GAPDH	F: CCATGGAGAAGGCTGGGG R: CAAAGTTGTCATGGATGACC	95, 8, 72 45 s, 30 s, 1 min

Table 1 (*continued*)

Genes	Primer sequence 5′–3′	PCR parameters[a]
CD81	F: CTCAACTGTTGTGGCTCCAAC R: CCAATGAGGTACAGCTTCCC	95, 55, 72 45 s, 30 s, 1 min
TLR3	F: GATCTGTCTCATAATGGCTTG R: GACAGATTCCGAATGCTTGTG	95, 55, 72 45 s, 30 s, 1 min
TLR7	F: CCAGACATCTCCCCAGCGTC R: GGCAAAACAGTAGGGACGGC	95, 55, 72 45 s, 30 s, 1 min
TLR8	F: CTGTGAGTTATGCGCCGAAG R: CGGGATTTCCGTTCTGGTGC	95, 55, 72 45 s, 30 s, 1 min
Myd88	F: GGTCTCCTCCACATCCTCCC R: CCAGCTTGGTAAGCAGCTCG	95, 55, 72 45 s, 30 s, 1 min
IRF3	F: GAACCCCAAAGCCACGGATC R: CCTCCCGGGAACATATGCAC	95, 55, 72 45 s, 30 s, 1 min
IRF7	F: GTGCTGTTCGGAGAGTGGCTC R: CAGCCCAGGCCTTGAAGATG	95, 55, 72 45 s, 30 s, 1 min

CYP, cytochrome P450; EGFR, epidermal growth factor receptor; F, forward primer; FGFR, fibroblast growth factor receptor; GAPDH, glyceraldehyde phosphate dehydrogenase; HGF, hepatocyte growth factor; HGFR, hepatocyte growth factor receptor; HNF, hepatocyte nuclear factor; HTF, human transferrin; IGF-1R, insulin-like growth factor-type I receptor; IRF, interferon regulatory factor; R, reverse primer; TGF, transforming growth factor; TGFR, transforming growth factor receptor; TLR, toll like receptor.

[a] Temperatures are tabulated in the first lane in degrees celsius and the corresponding times in the second lane. Performing one-step RT-PCR, reverse transcription was carried out at 42 °C for 20 min with a pre-PCR denaturation at 95 °C for 10 min.

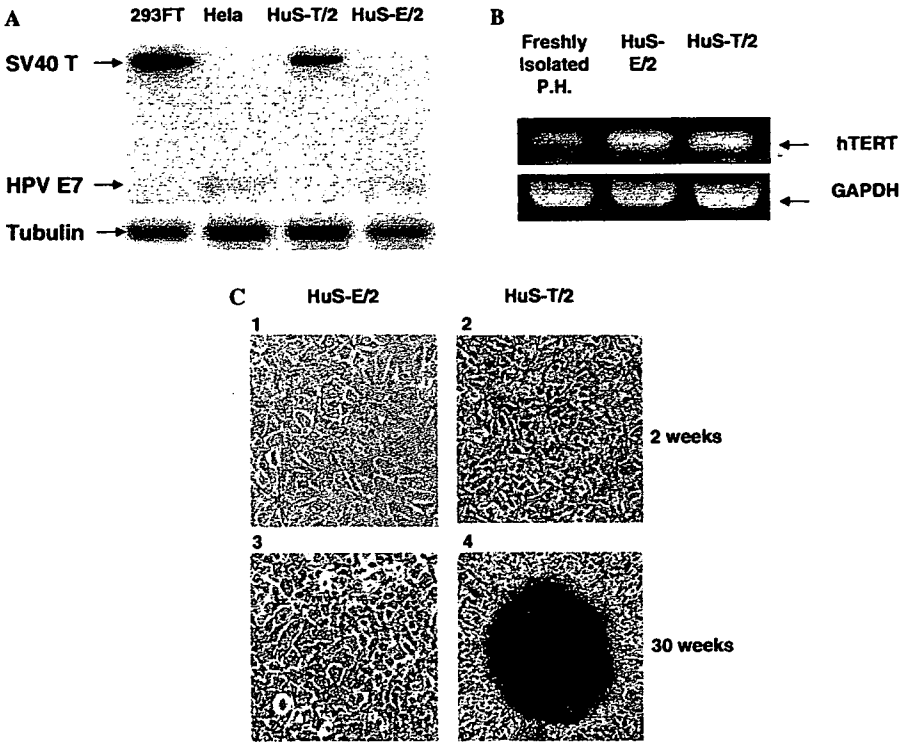

Fig. 1. (A) Immunoblot detection of SV40 T and HPV E7 expression in HuS-T/2 and HuS-E/2 cells, respectively. 293-FT and HeLa cells were used as positive controls for SV40 T and HPV E7 expression, respectively. The specific bands representing the targets are indicated. Detection of tubulin expression in all cells served as an internal control. (B) Human Telomerase Reverse Transcriptase (hTERT) expression was examined by RT-PCR in freshly isolated hepatocytes and the HuS-E/2 and HuS-T/2 cell lines. GAPDH expression was used as an internal control. The hTERT-specific bands are shown. (C) Morphological characteristics of HuS-E/2 and HuS-T/2 cells after two (panels 1 and 2) and 30 (panels 3 and 4) weeks in culture. [This figure appears in colour on the web.]

while the HPV18/E6E7-immortalized clones were named HuS-E cells and given numbers from 1 to 4. Expression of SV40 T and HPV E7 proteins was detected in the appropriate cells by immunoblot analysis (Fig. 1A). In both immortalized cell lines, expression of hTERT-mRNA was enhanced in comparison to non-transduced, freshly isolated hepatocytes as determined by RT-PCR (Fig. 1B). HuS-E cells were larger in size and exhibited slower growth than HuS-T cells (Fig. 1C).

3.2. Characterization of HuS-E and HuS-T immortalized hepatocytes

The HuS-E/2 and HuS-T/2 clones demonstrated the highest expression of hepatocyte-specific markers and transcription factors by RT-PCR (data not shown); these cells were used as representative for each group in this study. To address if HuS-E/2 and HuS-T/2 maintained similar characteristics as primary hepatocytes, they were both cultured continuously for 30 weeks and the expression profiles of a variety of growth factors (Fig. 2A), growth factor receptors (Fig. 2B), hepatocyte-specific nuclear factors (Fig. 2C), albumin, apolipoprotein-A1, transferrin (Fig. 2D), cytochrome p450 (CYP) genes (Fig. 2E), and GAPDH were compared with freshly isolated primary hepatocytes after isolation or two weeks of culture, Huh-7.5 cells, and 293 cells. After two weeks in culture, the expression of nearly all examined genes was similar between freshly isolated hepatocytes and the HuS-E/2 cell line. HuS-E/2 cells, however, exhibited higher expression of TGFβ2 (Fig. 2A), TGFβ2R, and HGFR (Fig. 2B) and lower expression of CYP 3A4 and 2C9 (Fig. 2E) in comparison to freshly isolated hepatocytes. Primary hepatocytes displayed reduced expression of TGFβ1 and TGFβ2 (Fig. 2A) and a loss of CYP1A1 expression (Fig. 2E) after two weeks of culture. HuS-E/2 cells exhibited higher expression of HGF (Fig. 2A), HGF receptor (Fig. 2B), HNF-4, (Fig. 2C), albumin, apolipoprotein-A1, HTF, and E-cadherin (Fig. 2D) in comparison to HuS-T/2 cells. Expression of CYP 3A4 (Fig. 2E) was lost from both HuS-T/2 and HuS-E/2 cells, while HuS-T/2 cells also lost the expression of HNF-1α (Fig. 2D), and CYPs 2B, 2E1 (Fig. 2E).

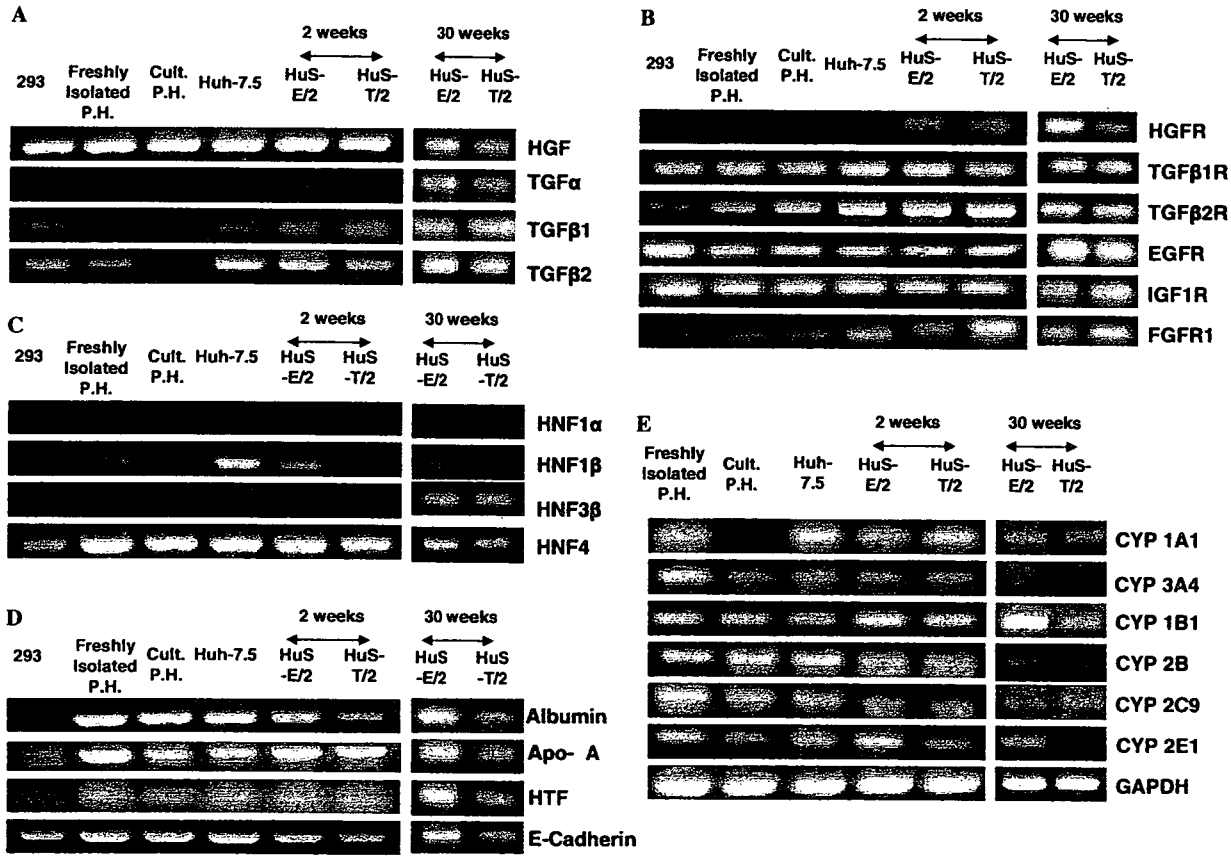

Fig. 2. Expression of the genes encoding growth factors (A), growth factor receptors (B), hepatocyte-specific nuclear factors (C), hepatocyte differentiation and functional markers (D), and CYP enzymes (E) in 293 cells, freshly isolated primary hepatocytes (P.H.), primary hepatocytes cultured for two weeks (Cult. P.H.), Huh-7.5 cells, and HuS-E/2 and HuS-T/2 cells cultured for two and 30 weeks were investigated by RT-PCR. The bands representing specific targets are indicated in the representative reactions.

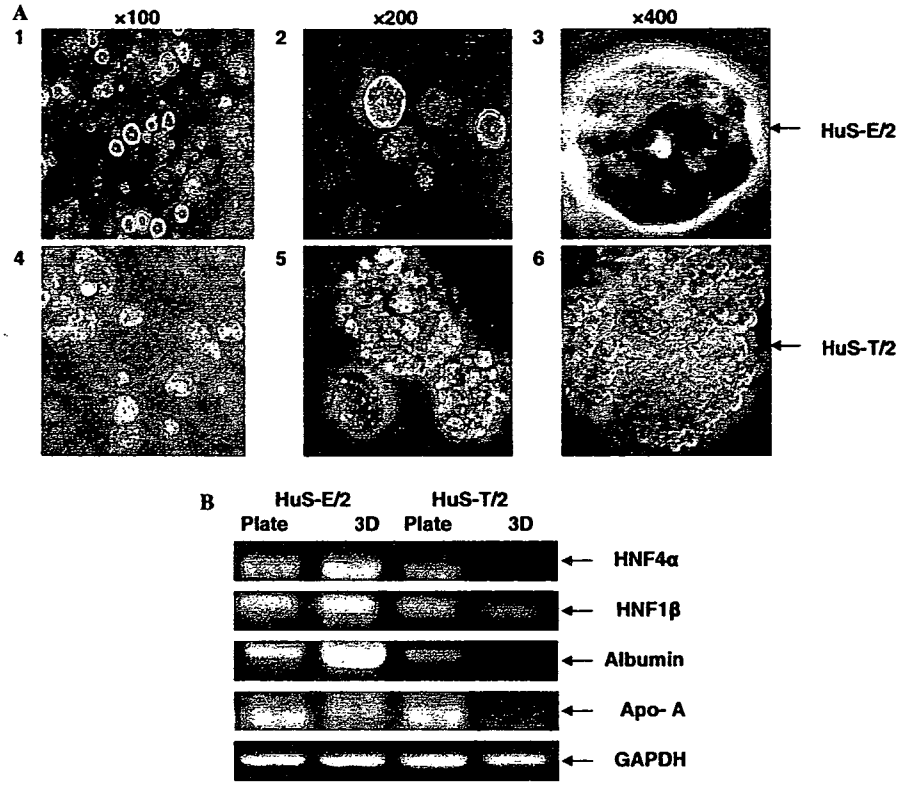

Fig. 3. (A) The morphology of HuS-E/2 and HuS-T/2 cells in 3D culture. HuSE/2 and HuS-T/2 cells were cultured in Mebiol Gel in 12-well plates at a concentration of 5×10^5 cells/well. The microscopic characteristics of these cells after one week of 3D culture are shown. (B) The expressions of HNF4α, HNF1β, albumin, and apo-A by HuS-E/2 and HuS-T/2 cells in both flat and 3D cultures are detailed. After one week of culture of HuS-E/2 and HuS-T/2 cells in flat and 3D cultures, the expressions of HNF4α, HNF1β, albumin, and apo-A were measured by RT-PCR in 250 ng total RNA.

HuS-T/2 but not in HuS-E/2 cells showed a transformed-like character starting from the 13th week of culture. This was demonstrated by continuing proliferation after confluence, pile-up formations (Fig. 1C), and proliferating in serum-deprevied condition. However, HuS-E/2 cells did not show any transformed-like characters even after 30 weeks of culture.

3.3. The characteristics of HuS-E and HuS-T immortalized hepatocytes in 3D culture

After one week in 3D culture, HuS-E/2 (Fig. 3A, panels 1, 2, and 3) cells adopted a donut-shaped structure with a central pore, while HuS-T/2 cells (Fig. 3A, panels 4, 5, and 6) displayed irregular mass formations (similar to the growth pattern of Huh-7.5 cells in 3D culture (data not shown)). In 3D culture, while the expression of HNF4, HNF1β, and albumin was enhanced in HuS-E/2, it was decreased in HuS-T/2 cells (Fig. 3B).

3.4. HCV infection to HuS-E/2

We further assessed the HCV infectivity of HuS-E- and HuS-T-derived clones by infection with HCV-1b-infected serum. Of the three HuS-E clones examined, HuS-E/2 clone demonstrated the highest infectability with HCV genotype 1b in comparison to Huh-7.5, PH5CH8 (Fig. 4A), and HuS-T cells (data not shown), which were excluded from further experiments.

3.5. Anti-CD81 blocked HCV infectivity

CD81 is involved in the entry of HCV pseudoparticles [24] and in vitro-synthesized JFH-1 [7]. To determine if authentic viral particles follow the same route of entry when infecting HuS-E/2 cells, we first examined the CD81 expression by RT-PCR. Both HuS-E/2 and HuS-T/2 cells expressed similar amounts of CD81 as freshly isolated hepatocytes and Huh-7.5 cells (Fig. 4B). Antibodies against CD81 reduced HCV infectivity of HuS-E/2 cells from the levels seen using a non-specific control antibody, confirming the importance of CD81 in HCV infectivity (Fig. 4C).

3.6. IFNα blocked HCV infectivity

We treated HuS-E/2 cells with HCV-containing serum. Cells were then cultured in fresh medium supplemented